INTERNATIONAL JOURNAL FOR NUMERICAL METHODS IN FLUIDS, VOL. 14, 1173–1191 (1992)

A GENERAL NUMERICAL METHOD FOR SOLUTION OF GRAVITY WAVE PROBLEMS. PART 2: STEADY NON-LINEAR GRAVITY WAVES

S. J. LIAO*

Institute of Shipbuilding, University of Hamburg, Laemmersieth 90, D-2000 Hamburg 60, Germany

SUMMARY

A type of numerical scheme for 2D and 3D steady non-linear water wave problems is described. It is based on the finite process method and is insensitive to initial solutions. The relationship between the finite process method and iterative techniques is discussed. As a numerical example the flow past a submerged vortex is solved and the results are compared with those of other authors.

KEY WORDS Steady non-linear water waves Potential flow Continuous mapping

1. INTRODUCTION

Steady potential flow with a free surface is a typical non-linear problem. In 1977 Dawson[1] gave a numerical scheme for ship wave problems which was based on the singularity distribution method developed by Hess and Smith[2] in 1962. He distributed the simple singularities on the surface of double-model ship and also on the limited region of the undisturbed free surface around the ship. Linear free surface conditions were used and a type of four-point upwind operator was applied to treat the radiation condition. Many researchers[3–8] have since expanded the basic idea of Dawson to study water wave problems with non-linear free surface conditions. In order to treat the non-linear free surface conditions, some of these used the perturbation expansion technique and neglected the non-linear terms of perturbation in the non-linear free surface conditions. In this way several iterative numerical schemes were given. However, as mentioned by Macarthur,[9] nearly all iterative formulae are sensitive not only to the initial solutions but also to the number of unknowns.

In Reference 10 a type of general numerical method for non-linear problems, called the finite process method (FPM), is described. Since it is based on continuous mapping, the FPM can successfully avoid the use of iterative techniques and is insensitive not only to the initial solutions but also to the number of unknowns. However, more CPU time is needed. In Reference 10 a numerical scheme for non-linear wave problems was derived and, as an example, the 2D non-linear progressive gravity wave in shallow water was solved by means of a finite Fourier series. The numerical results were in good agreement with those of other authors.

The present work is a continuation of Reference 10. The basic ideas given in Reference 10 are expanded to give a type of numerical scheme for 2D and 3D steady potential flows with non-linear free surface conditions. Instead of using finite Fourier series, simple sources ($1/r$ for 3D problems and $\ln r$ for 2D problems) are used. The relationship between the FPM and iterative techniques is investigated.

*Current address: Institute of Underwater Engineering, Shanghai Jiao Tong University, Shanghai 200030, P.R. China

0271–2091/92/101173–19$09.50

Received March 1991
Revised October 1991

2. MATHEMATICAL DESCRIPTION

Steady water wave problems can be generally described by

$$\nabla^2\phi(x, y, z)=0 \quad \text{in } \Omega, \tag{1}$$

with the non-linear free surface conditions

$$g\phi_z+\tfrac{1}{2}\nabla\phi\nabla(\nabla\phi\nabla\phi)=0 \quad \text{on } z=\zeta(x, y), \tag{2}$$

$$\zeta=\frac{1}{2g}(U^2-\nabla\phi\nabla\phi) \quad \text{on } z=\zeta(x, y) \tag{3}$$

and the boundary condition on body ∂B

$$\left.\frac{\partial\phi}{\partial n}\right|_{\partial B}=0, \tag{4}$$

where $\phi(x, y, z)$ is the velocity potential function, $\zeta(x, y)$ is the wave elevation, g is the gravitational acceleration and U is the velocity of the body. The co-ordinate system $Oxyz$ with z positive upwards is moving at the same velocity U as the body.

For simplicity we define

$$\mathscr{R}(\phi)=g\phi_z+\tfrac{1}{2}\nabla\phi\nabla(\nabla\phi\nabla\phi), \tag{5}$$

$$\mathscr{Z}(\phi)=\frac{1}{2g}(U^2-\nabla\phi\nabla\phi). \tag{6}$$

3. FINITE PROCESS METHOD

One can find two continuous functions $f_1(p)$ and $f_2(p)$ in $p\in[0, 1]$, called first- and second-type process functions respectively, which satisfy

$$f_1(p)=\begin{cases}0 & \text{when } p=0,\\ 1 & \text{when } p=1,\end{cases} \tag{7}$$

$$f_2(p)=\begin{cases}1 & \text{when } p=0,\\ 0 & \text{when } p=1.\end{cases} \tag{8}$$

Then a continuous mapping $\phi(x, y, z)\to\phi(x, y, z; p)$, $\zeta(x, y)\to\zeta(x, y; p)$, $\Omega\to\Omega(p)$ can be obtained as

$$\nabla^2\phi(x, y, z; p)=0 \quad \text{in } \Omega(p), \tag{9}$$

with boundary conditions

$$f_1(p)\mathscr{R}(\phi)+f_2(p)[\mathscr{R}(\phi)-\mathscr{R}(\phi_0)]=0 \quad \text{on } z=\zeta(x, y; p), \tag{10}$$

$$\zeta(x, y; p)=f_1(p)\mathscr{Z}(\phi)+f_2(p)\zeta_0(x, y) \quad \text{on } z=\zeta(x, y; p), \tag{11}$$

$$\left.\frac{\partial\phi(x, y, z; p)}{\partial n}\right|_{\partial B}=0, \tag{12}$$

where $\zeta_0(x, y)$ is an initial wave elevation and $\phi_0(x, y, z)$ is an initial velocity potential function which satisfies

$$\nabla^2\phi_0(x, y, z)=0 \quad \text{in } \Omega_0 \tag{13}$$

and the boundary condition

$$\left.\frac{\partial \phi_0}{\partial n}\right|_{\partial B}=0. \tag{14}$$

If $p=0$, then $f_1(p)=0$ and $f_2(p)=1$. Hence from (9)–(12) one has the *initial equation*

$$\nabla^2\phi(x, y, z; 0)=0 \quad \text{in } \Omega(0), \tag{15}$$

with boundary conditions

$$\mathscr{R}(\phi)=\mathscr{R}(\phi_0) \qquad \text{on } z=\zeta(x, y; 0), \tag{16}$$

$$\zeta(x, y; 0)=\zeta_0(x, y) \qquad \text{on } z=\zeta(x, y; 0), \tag{17}$$

$$\left.\frac{\partial \phi(x, y, z; 0)}{\partial n}\right|_{\partial B}=0. \tag{18}$$

Let $\zeta(x, y; 0)=\zeta_0(x, y)$; then (17) is satisfied. It is interesting that $\phi_0(x, y, z)$ determined by (13) and (14) is just the solution of initial equation (15), (16) and (18); therefore

$$\phi(x, y, z; 0)=\phi_0(x, y, z), \tag{19}$$

$$\zeta(x, y; 0)=\zeta_0(x, y), \tag{20}$$

$$\Omega(0)=\Omega_0. \tag{21}$$

When $p=1, f_1(p)=1$ and $f_2(p)=0$. Hence from (9)–(12) one obtains the *final equation*

$$\nabla^2\phi(x, y, z; 1)=0 \quad \text{in } \Omega(1), \tag{22}$$

with boundary conditions

$$\mathscr{R}(\phi)=0 \qquad \text{on } z=\zeta(x, y; 1), \tag{23}$$

$$\zeta(x, y; 1)=\mathscr{L}(\phi) \qquad \text{on } z=\zeta(x, y; 1), \tag{24}$$

$$\left.\frac{\partial \phi(x, y, z; 1)}{\partial n}\right|_{\partial B}=0. \tag{25}$$

The final equations (22)–(25) are just the same as the original equations (1)–(4) respectively. Suppose the solutions of the original equations (1)–(4) are $\phi_f(x, y, z)$ and $\zeta_f(x, y)$, called the final solutions. Then one has the relations

$$\phi_f(x, y, z)=\phi(x, y, z; 1), \tag{26}$$

$$\zeta_f(x, y)=\zeta(x, y; 1). \tag{27}$$

From the above analysis one can see that the continuous mapping determined by (9)–(12) gives relations between the selected initial solutions $\phi_0(x, y, z)$ and $\zeta_0(x, y)$ and the final solutions $\phi_f(x, y, z)$ and $\zeta_f(x, y)$ which can be described in the form of integrals as

$$\begin{aligned}\phi_f(x, y, z)&=\phi(x, y, z; 1)\\ &=\phi(x, y, z; 0)+\int_0^1 \phi^{[1]}(x, y, z; p)\mathrm{d}p\\ &=\phi_0(x, y, z)+\int_0^1 \phi^{[1]}(x, y, z; p)\mathrm{d}p,\end{aligned} \tag{28}$$

$$\begin{aligned}\zeta_f(x, y) &= \zeta(x, y; 1) \\ &= \zeta(x, y; 0) + \int_0^1 \zeta^{[1]}(x, y; p)\mathrm{d}p \\ &= \zeta_0(x, y) + \int_0^1 \zeta^{[1]}(x, y; p)\mathrm{d}p, \end{aligned} \tag{29}$$

where

$$\phi^{[1]}(x, y, z; p) = \frac{\partial \phi(x, y, z; p)}{\partial p} \tag{30}$$

and

$$\zeta^{[1]}(x, y; p) = \frac{\partial \zeta(x, y; p)}{\partial p} \tag{31}$$

are first-order partial derivatives of $\phi(x, y, z; p)$ and $\zeta(x, y; p)$ with respect to p respectively.

For simplicity call equations (9)–(12) the zero-order process equations, the continuous mappings $\phi(x, y, z; p)$ and $\zeta(x, y; p)$ the zero-order processes of the velocity potential function and wave elevation respectively and $\phi^{[1]}(x, y, z; p)$ and $\zeta^{[1]}(x, y; p)$ the first-order process derivatives of $\phi(x, y, z; p)$ and $\zeta(x, y; p)$ respectively.

The first-order process derivatives $\phi^{[1]}(x, y, z; p)$ and $\zeta^{[1]}(x, y; p)$ can be obtained in the following way.

Deriving (9) and (12) with respect to p, one obtains

$$\frac{\partial}{\partial p}(\nabla^2 \phi) = \nabla^2\left(\frac{\partial \phi}{\partial p}\right) = \nabla^2 \phi^{[1]} = 0 \quad \text{in } \Omega(p), \tag{32}$$

$$\left.\frac{\partial \phi^{[1]}}{\partial n}\right|_{\partial B} = 0. \tag{33}$$

Deriving equation (10) with respect to p, one has

$$f_1'(p)\mathscr{R}(\phi) + f_2'(p)[\mathscr{R}(\phi) - \mathscr{R}(\phi_0)] + [f_1(p) + f_2(p)]\frac{\mathrm{d}\mathscr{R}(\phi)}{\mathrm{d}p} = 0 \quad \text{on } z = \zeta(x, y; p). \tag{34}$$

In the same way, deriving (11) with respect to p, one obtains

$$\zeta^{[1]}(x, y; p) = f_1'(p)\mathscr{Z}(\phi) + f_1(p)\frac{\mathrm{d}\mathscr{Z}(\phi)}{\mathrm{d}p} + f_2'(p)\zeta_0(x, y) \quad \text{on } z = \zeta(x, y; p). \tag{35}$$

Because the wave elevation $z = \zeta(x, y; p)$ is also a function of p, one has

$$\frac{\mathrm{d}\mathscr{R}}{\mathrm{d}p} = \frac{\partial \mathscr{R}}{\partial p} + \frac{\partial \mathscr{R}}{\partial z}\frac{\partial z}{\partial p} = \frac{\partial \mathscr{R}}{\partial p} + \frac{\partial \mathscr{R}}{\partial z}\zeta^{[1]} \qquad \text{on } z = \zeta(x, y; p), \tag{36}$$

$$\frac{\mathrm{d}\mathscr{Z}}{\mathrm{d}p} = \frac{\partial \mathscr{Z}}{\partial p} + \frac{\partial \mathscr{Z}}{\partial z}\frac{\partial z}{\partial p} = \frac{\partial \mathscr{Z}}{\partial p} + \frac{\partial \mathscr{Z}}{\partial z}\zeta^{[1]} \qquad \text{on } z = \zeta(x, y; p). \tag{37}$$

Substituting (37) into (35), one obtains

$$\zeta^{[1]}(x, y; p) = \frac{f_1'(p)\mathscr{Z}[\phi(x, y, z; p)] + f_2'(p)\zeta_0(x, y) + f_1(p)\partial\mathscr{Z}[\phi(x, y, z; p)]/\partial p}{1 - f_1(p)\partial\mathscr{Z}[\phi(x, y, z; p)]/\partial z} \quad \text{on } z = \zeta(x, y; p). \tag{38}$$

Substituting (36) and (38) into (34), one obtains

$$\frac{\partial \mathscr{R}}{\partial p}+f_1(p)\mathscr{S}(\phi; p)\frac{\partial \mathscr{Z}}{\partial p}=\mathscr{T}(\phi; p) \quad \text{on } z=\zeta(x, y; p), \tag{39}$$

where

$$\mathscr{S}[\phi(x, y, z; p); p]=\frac{\partial \mathscr{R}[\phi(x, y, z; p)]/\partial z}{1-f_1(p)\partial \mathscr{Z}[\phi(x, y, z; p)]/\partial z} \quad \text{on } z=\zeta(x, y; p), \tag{40}$$

$$\begin{aligned}\mathscr{T}[\phi(x, y, z; p); p]=&\frac{f_2'(p)\mathscr{R}[\phi_0(x, y, z)]-[f_1'(p)+f_2'(p)]\mathscr{R}[\phi(x, y, z; p)]}{f_1(p)+f_2(p)}\\ &-\mathscr{S}[\phi(x, y, z; p); p]\{f_1'(p)\mathscr{Z}[\phi(x, y, z; p)]+f_2'(p)\zeta_0(x, y)\}\\ &\text{on } z=\zeta(x, y; p).\end{aligned} \tag{41}$$

For simplicity, selecting $f_1(p)=p, f_2(p)=1-p$ and substituting

$$\frac{\partial \mathscr{R}}{\partial p}=g\phi_z^{[1]}+\tfrac{1}{2}\nabla\phi^{[1]}\nabla(\nabla\phi\nabla\phi)+\nabla\phi\nabla(\nabla\phi\nabla\phi^{[1]}), \tag{42}$$

$$\frac{\partial \mathscr{Z}}{\partial p}=-\frac{\nabla\phi\nabla\phi^{[1]}}{g} \tag{43}$$

and

$$\frac{\partial \mathscr{Z}}{\partial z}=-\frac{\nabla\phi\nabla\phi_z}{g} \tag{44}$$

into (38) and (39), one has the equations of $\phi^{[1]}(x, y, z; p)$ and $\zeta^{[1]}(x, y; p)$ as follows:

$$\begin{aligned}&g\phi_z^{[1]}+\tfrac{1}{2}\nabla\phi^{[1]}\nabla(\nabla\phi\nabla\phi)+\nabla\phi\nabla(\nabla\phi\nabla\phi^{[1]})-\frac{p\mathscr{S}(\phi; p)\nabla\phi\nabla\phi^{[1]}}{g}\\ &\quad=-\mathscr{R}(\phi_0)-\mathscr{S}(\phi; p)[\mathscr{Z}(\phi)-\zeta_0(x, y)] \quad \text{on } z=\zeta(x, y; p),\end{aligned} \tag{45}$$

$$\zeta^{[1]}(x, y; p)=\frac{\mathscr{Z}(\phi)-\zeta_0(x, y)-p\nabla\phi\nabla\phi^{[1]}/g}{1+p\nabla\phi\nabla\phi_z/g} \quad \text{on } z=\zeta(x, y; p), \tag{46}$$

where

$$\mathscr{S}(\phi; p)=\frac{\partial \mathscr{R}/\partial z}{1+p\nabla\phi\nabla\phi_z/g} \quad \text{on } z=\zeta(x, y; p). \tag{47}$$

The system consisting of equations (32), (33), (45) and (46) is linear with respect to $\phi^{[1]}(x, y, z; p)$ and $\zeta^{[1]}(x, y; p)$. If $\phi(x, y, z; p)$ and $\zeta(x, y; p)$ are known, then $\phi^{[1]}(x, y, z; p)$ and $\zeta^{[1]}(x, y; p)$ can be obtained by solving this system of linear equations. Thus $\phi(x, y, z; p+\Delta p)$ and $\zeta(x, y; p+\Delta p)$ can be obtained by using the Runge–Kutta method in the process domain $p\in[0, 1]$ as follows:

$$\phi(x, y, z; p+\Delta p)=\phi(x, y, z; p)+\tfrac{1}{6}(k_1+2k_2+2k_3+k_4), \tag{48}$$

$$\zeta(x, y; p+\Delta p)=\zeta(x, y; p)+\tfrac{1}{6}(m_1+2m_2+2m_3+m_4), \tag{49}$$

where

$$k_1=\Delta p\phi^{[1]}[\phi(x, y, z; p), \zeta(x, y; p); p], \tag{50}$$

$$m_1=\Delta p\zeta^{[1]}[\phi(x, y, z; p), \zeta(x, y; p); p], \tag{51}$$

$$k_2 = \Delta p \phi^{[1]}[\phi(x, y, z; p) + k_1/2,\ \zeta(x, y; p) + m_1/2;\ p + \Delta p/2], \tag{52}$$

$$m_2 = \Delta p \zeta^{[1]}[\phi(x, y, z; p) + k_1/2,\ \zeta(x, y; p) + m_1/2;\ p + \Delta p/2], \tag{53}$$

$$k_3 = \Delta p \phi^{[1]}[\phi(x, y, z; p) + k_2/2,\ \zeta(x, y; p) + m_2/2;\ p + \Delta p/2], \tag{54}$$

$$m_3 = \Delta p \zeta^{[1]}[\phi(x, y, z; p) + k_2/2,\ \zeta(x, y; p) + m_2/2;\ p + \Delta p/2], \tag{55}$$

$$k_4 = \Delta p \phi^{[1]}[\phi(x, y, z; p) + k_3,\ \zeta(x, y; p) + m_3;\ p + \Delta p], \tag{56}$$

$$m_4 = \Delta p \zeta^{[1]}[\phi(x, y, z; p) + k_3,\ \zeta(x, y; p) + m_3;\ p + \Delta p]. \tag{57}$$

Note that the final results are obtained at $p = 1$.

4. SIMPLE NUMERICAL EXAMPLES

The 2D potential flow past a submerged vortex is a simple but typical non-linear problem.* As shown in Figure 1, the vortex is submerged at $(0, -b)$ with circulation Γ. Upstream there exists a uniform stream with velocity U. Downstream there exists a steady wave with wavelength λ_w. In the case of finite water depth, Salvesen and Kerczek[11] solved this problem by an iterative finite difference technique and compared their numerical results with their perturbation solutions in deep water. Similarly to Salvesen and Kerczek,[11] we select a uniform stream velocity $U = 10$ ft s^{-1} and a vortex submergence $b = 4{\cdot}5$ ft,† but the water depth is infinite so that more rigorous comparison with perturbation solutions in deep water can be made.

Similarly to Jensen *et al.*,[6] we use the singularity distribution method to solve the corresponding equations (32), (33), (45) and (46). The simple sources $\ln r$ are distributed continuously at a distance h_s above the undisturbed water surface in the limited region $\overline{AB}$: $x_a \leqslant x \leqslant x_b$ shown in Figure 1. We select $h_s > \zeta_{max} = U^2/2g$ in order to let the simple sources on $\overline{AB}$ be always above the wave elevation.

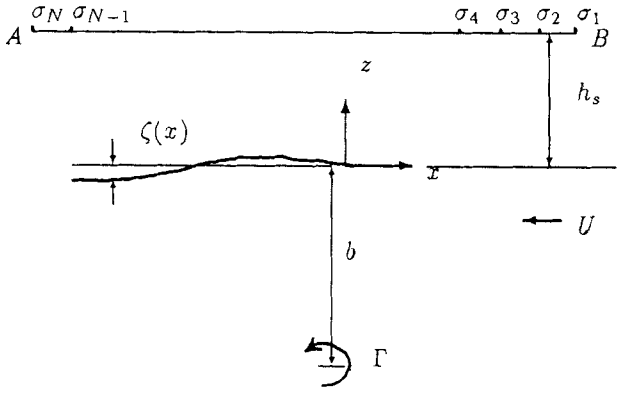

Figure 1. Co-ordinate system and grid for numerical computation

* We have two reasons for selecting this problem as an example even though it seems too simple from the viewpoint of engineering. First, the main purpose of this paper is to examine the basic idea of a type of numerical method. Secondly, there exist detailed numerical results for this problem given by other authors so that comparisons can be made.

† For ease of comparison with the results of Reference 11 we use the British system of units, where 1 ft ≡ 0·3048 m and 1 lb ≡ 0·454 kg.

The treatment of the radiation condition seems even more difficult than that of the non-linear free surface conditions. Several numerical techniques (or, more precisely, several numerical arts) have been used to treat the radiation condition. The method used in Reference 6 seems efficient and very simple, although its mathematical meaning is not very clear. In this paper we use the same technique as given in Reference 6 to treat the radiation condition, i.e.

$$\xi_i = x_i - \delta x \quad (i = 1, 2, 3, \ldots, N),$$

where (x_i, ζ_i) are co-ordinates of points on the wave elevation, (ξ_i, h_s) are co-ordinates of points on $\overline{AB}$ and $\delta x = |x_i - x_{i+1}|$ is a selected constant.

Using

$$\phi_0(x, z) = -Ux + \frac{\Gamma}{2\pi}\tan^{-1}\left(\frac{z+b}{x}\right) - \frac{\Gamma}{2\pi}\tan^{-1}\left(\frac{z-b}{x}\right) \tag{58}$$

as the initial velocity potential function and $\zeta_0(x) = 0$ as the initial wave elevation, the corresponding continuous mapping $\phi(x, z; p)$ can be described as

$$\begin{aligned}\phi(x, z; p) &= \phi_0(x, z) + \int_{x_a}^{x_b} \sigma(\xi, h_s; p) \ln\{\sqrt{[(x-\xi)^2 + (z-h_s)^2]}\}\, d\xi \\ &= \phi_0(x, z) + \sum_{m=1}^{N} \varphi(x - \xi_m, z)\sigma_m(p),\end{aligned} \tag{59}$$

where $\sigma_m(p) = \sigma(\xi_m, h_s; p)$ $(m = 1, 2, \ldots, N)$. Then the first-order process derivatives $\phi^{[1]}(x, z; p)$ can be expressed as

$$\begin{aligned}\phi^{[1]}(x, z; p) &= \int_{x_a}^{x_b} \sigma^{[1]}(\xi, h_s; p) \ln\{\sqrt{[(x-\xi)^2 + (z-h_s)^2]}\}\, d\xi \\ &= \sum_{m=1}^{N} \varphi(x - \xi_m, z)\sigma_m^{[1]}(p).\end{aligned} \tag{60}$$

Clearly, $\phi^{[1]}(x, z; p)$ described above satisfies (32).

From expression (60) one easily obtains

$$\phi_x^{[1]}(x, z; p) = \sum_{m=1}^{N} \varphi_x(x - \xi_m, z)\sigma_m^{[1]}(p), \tag{61}$$

$$\phi_z^{[1]}(x, z; p) = \sum_{m=1}^{N} \varphi_z(x - \xi_m, z)\sigma_m^{[1]}(p), \tag{62}$$

$$\phi_{xx}^{[1]}(x, z; p) = \sum_{m=1}^{N} \varphi_{xx}(x - \xi_m, z)\sigma_m^{[1]}(p), \tag{63}$$

$$\phi_{xz}^{[1]}(x, z; p) = \sum_{m=1}^{N} \varphi_{xz}(x - \xi_m, z)\sigma_m^{[1]}(p). \tag{64}$$

Substituting (61)–(64) in (45), one obtains the set of linear algebraic equations of $\sigma_m^{[1]}$ $(m = 1, 2, \ldots, N)$ as follows:

$$\mathbf{E}(p)\sigma^{[1]}(p) = \mathbf{t}(p). \tag{65}$$

Here

$$\mathbf{E}(p)=\{e_{ij}(p)\} \qquad (i,j=1,2,\ldots,N),$$
$$\sigma^{[1]}(p)=\{\sigma_m^{[1]}(p)\} \qquad (m=1,2,\ldots,N),$$
$$\mathbf{t}(p)=\{\mathscr{T}_m(p)\} \qquad (m=1,2,\ldots,N),$$

with

$$e_{ij}(p)=b_1(x_i,z_i;p)\varphi_x(x_i-\xi_j,z_i)+b_2(x_i,z_i;p)\varphi_z(x_i-\xi_j,z_i)$$
$$+b_3(x_i,z_i;p)\varphi_{xx}(x_i-\xi_j,z_i)+b_4(x_i,z_i;p)\varphi_{xz}(x_i-\xi_j,z_i) \quad \text{on } z_i=\zeta(x_i;p), \tag{66}$$

where

$$b_1(x,z;p)=2(\phi_x\phi_{xx}+\phi_z\phi_{xz})-p\mathscr{S}(\phi;p)\phi_x/g \qquad \text{on } z=\zeta(x;p), \tag{67}$$
$$b_2(x,z;p)=g+2(\phi_x\phi_{xz}-\phi_z\phi_{xx})-p\mathscr{S}(\phi;p)\phi_z/g \quad \text{on } z=\zeta(x;p), \tag{68}$$
$$b_3(x,z;p)=\phi_x^2-\phi_z^2 \quad \text{on } z=\zeta(x;p), \tag{69}$$
$$b_4(x,z;p)=2\phi_x\phi_z \qquad \text{on } z=\zeta(x;p), \tag{70}$$
$$\mathscr{T}_m(p)=-\mathscr{R}[\phi_0(x_m,z_m)]-\mathscr{S}[\phi(x_m,z_m;p);p]\{\mathscr{L}[\phi(x_m,z_m;p)]-\zeta_0(x_m)\}$$
$$\text{on } z_m=\zeta(x_m;p) \quad (m=1,2,\ldots,N). \tag{71}$$

We solve the set of linear algebraic equations (65) by the Gauss–Jordan elimination method. After $\phi^{[1]}(x,z;p)$ is known, $\zeta^{[1]}(x;p)$ can be easily obtained from expression (46). Note that $\phi(x,z;p+\Delta p)$ and $\zeta(x;p+\Delta p)$ are obtained by the Runge–Kutta method, shown as expressions (48)–(57).

The final solution $\phi_f(x,z)$ is

$$\phi_f(x,z)=\phi_0(x,z)+\int_{x_a}^{x_b}\sigma_f(\xi,h_s)\ln\{\sqrt{[(x-\xi)^2+(z-h_s)^2]}\}\,d\xi$$
$$=-Ux+\phi^*(x,z), \tag{72}$$

where

$$\sigma_f(\xi,h_s)=\int_0^1\sigma^{[1]}(\xi,h_s;p)dp \tag{73}$$

or, more precisely,

$$\sigma_f(\xi_m,h_s)=\int_0^1\sigma_m^{[1]}(p)dp \quad (m=1,2,\ldots,N). \tag{74}$$

Note that the $\sigma_m(p+\Delta p)$ $(m=1,2,\ldots,N)$ are also obtained by the Runge–Kutta method.

Let

$$(e_d)_{\max}=\max_{1\leqslant i\leqslant N}\frac{g|\zeta_f(x_i)-\mathscr{L}(\phi_f)|}{U^2} \quad \text{on } z_i=\zeta_f(x_i) \tag{75}$$

and

$$(e_k)_{\max}=\max_{1\leqslant i\leqslant N}\frac{|\mathscr{R}(\phi_f)|}{gU} \qquad \text{on } z_i=\zeta_f(x_i) \tag{76}$$

denote the maximum non-dimensional errors of the non-linear dynamic and kinematic free surface conditions respectively.

The exact wave resistance formula for two-dimensional potential flow, neglecting surface tension, is[12]

$$R_w=\tfrac{1}{2}\rho\int_{-\infty}^{\zeta(x_0)}\{[\phi_z^*(x_0,z)]^2-[\phi_x^*(x_0,z)]^2\}\,dz+\tfrac{1}{2}g\rho\zeta^2(x_0), \tag{77}$$

where the plane $x=x_0$ may be taken at any distance behind the submerged vortex, i.e. $x_0<0$. R_w can be obtained by numerical integral.

As a test computation let us consider the flow past the submerged vortex $\Gamma/2\pi=2{\cdot}20\ \text{ft}^2\,\text{s}^{-1}$, corresponding to a strong non-linear problem.

Select $h_s=1{\cdot}6$ ft, $N=80$, $x_a=-2{\cdot}5\lambda_0$ and $x_b=1{\cdot}5\lambda_0$, where $\lambda_0=2\pi U^2/g=19{\cdot}54$ ft. The corresponding maximum initial errors are $(e_{k0})_{max}=5{\cdot}1\times10^{-2}$ and $(e_{d0})_{max}=0{\cdot}1$. The results obtained for different values of Δp are given in Table I.

It is clear from Table I that the smaller Δp is, the more accurate the numerical results are. In the case $\Delta p=0{\cdot}1$ the numerical results appear to be accurate enough. This means that sufficiently accurate results can be obtained by the FPM if a small enough value of Δp is used. Thus no iterative techniques are needed, although more CPU time will be used.

Using the FPM, reasonable and accurate numerical results can be obtained in the region $-6{\cdot}49\leqslant\Gamma/2\pi\leqslant2{\cdot}5\ \text{ft}^2\,\text{s}^{-1}$.

For simplicity we have selected in this paper $f_1(p)=p$ and $f_2(p)=1-p$. Clearly, there exists many other process functions, e.g.

$$f_1(p)=\sin^m\left(\frac{p\pi}{2}\right)\quad(m\geqslant1),\qquad f_2(p)=\cos^m\left(\frac{p\pi}{2}\right)\quad(m\geqslant1)$$

or

$$f_1(p)=p^m,\qquad f_2(p)=(1-p)^m.$$

Using these process functions in our computer programme, we obtain a similar result, i.e. the smaller Δp is, the more accurate the numerical results are.

5. RELATIONSHIP BETWEEN FINITE PROCESS METHOD AND ITERATION

Consider the zero-order process equations (9)–(12). Clearly, the initial solutions $\phi_0(x,z)$ and $\zeta_0(x)$ can be freely selected. If $\phi_0(x,z)$ and $\zeta_0(x)$ are just the true solutions of the original problem, then according to the first-order process equations (32), (33), (45) and (46), $\phi^{[1]}(x,z;p)=0$ and

Table I. Numerical results for different values of Δp

Δp	ζ_{max} (ft)	ζ_{min} (ft)	λ_w (ft)	R_w (lb ft^{-1})	$(e_k)_{max}$	$(e_d)_{max}$
1	0·9342	−0·7201	18·3512	9·4341	$1{\cdot}6\times10^{-2}$	$8{\cdot}1\times10^{-3}$
1/2	0·9314	−0·7289	18·3613	9·5473	$2{\cdot}5\times10^{-3}$	$1{\cdot}6\times10^{-3}$
1/5	0·9329	−0·7301	18·3651	9·5787	$5{\cdot}5\times10^{-4}$	$1{\cdot}5\times10^{-4}$
1/10	0·9334	−0·7301	18·3644	9·5789	$7{\cdot}5\times10^{-5}$	$1{\cdot}2\times10^{-5}$
1/20	0·9334	−0·7301	18·3644	9·5778	$1{\cdot}1\times10^{-5}$	$7{\cdot}8\times10^{-7}$
1/50	0·9334	−0·7301	18·3644	9·5774	$4{\cdot}8\times10^{-7}$	$2{\cdot}6\times10^{-8}$
1/100	0·9334	−0·7301	18·3644	9·5774	$3{\cdot}5\times10^{-8}$	$7{\cdot}7\times10^{-9}$

$\zeta^{[1]}(x; p)=0$. However, at the beginning of the computation the solutions are unknown and we must select initial solutions which may be far from the accurate solutions. The general form of the initial solution $\phi_0(x, z)$ can be written as

$$\phi_0(x, z)=-Ux+\frac{\Gamma}{2\pi}\tan^{-1}\left(\frac{z+b}{x}\right)-\frac{\Gamma}{2\pi}\tan^{-1}\left(\frac{z-b}{x}\right)+\int_{x_a}^{x_b}\sigma_0(\xi, h_s)\ln\{\sqrt{[(x-\xi)^2+(z-h_s)^2]}\}\,d\xi \tag{78}$$

The corresponding final solution $\phi_f(x, z)$ is now

$$\phi_f(x, z)=-Ux+\frac{\Gamma}{2\pi}\tan^{-1}\left(\frac{z+b}{x}\right)-\frac{\Gamma}{2\pi}\tan^{-1}\left(\frac{z-b}{x}\right)+\int_{x_a}^{x_b}\sigma_f(\xi, h_s)\ln\{\sqrt{[(x-\xi)^2+(z-h_s)^2]}\}\,d\xi, \tag{79}$$

where

$$\sigma_f(\xi, h_s)=\sigma_0(\xi, h_s)+\int_0^1\sigma^{[1]}(\xi, h_s; p)dp \tag{80}$$

or, more clearly,

$$\sigma_f(\xi_m, h_s)=\sigma_0(\xi_m, h_s)+\int_0^1\sigma_m^{[1]}(p)dp \quad (m=1, 2, \ldots, N). \tag{81}$$

At the beginning of the computation select $\sigma_0(\xi, h_s)=0$ and $\zeta_0(x)=0$ to make a computation under a selected Δp. If Δp is small enough, the results are sufficiently accurate, which can be used as the solution of the original problem. If Δp is not small enough, then crude results $\sigma_f^*(\xi, h_s)$ and $\zeta_f^*(x)$ are obtained. Although $\sigma_f^*(\xi, h_s)$ and $\zeta_f^*(x)$ are not accurate enough, they are clearly much better than the selected initial solutions $\sigma_0(\xi, h_s)=0$ and $\zeta_0(x)=0$. Clearly, better numerical results will be obtained if $\sigma_f^*(\xi, h_s)$ and $\zeta_f^*(x)$ are used as new initial solutions to make a new computation. This is in fact just the idea of iteration. From the view point of this, expressions

Table II. Iterations for different values of Δp

Δp	Iterations	ζ_{max}(ft)	ζ_{min} (ft)	λ_w (ft)	R_w (lb ft^{-1})	$(e_k)_{max}$	$(e_d)_{max}$
	1	0·9341	−0·7201	18·3512	9·4341	1.6×10^{-2}	$8\cdot1\times10^{-3}$
1	2	0·9334	−0·7301	18·3644	9·5774	$3\cdot6\times10^{-6}$	$4\cdot3\times10^{-6}$
	3	0·9334	−0·7301	18·3644	9·5774	$2\cdot7\times10^{-13}$	$2\cdot2\times10^{-13}$
	4	0·9334	−0·7301	18·3644	9·5774	$8\cdot1\times10^{-16}$	$2\cdot2\times10^{-16}$
	1	0·9329	−0·7301	18·3651	9·5787	$5\cdot5\times10^{-4}$	$1\cdot5\times10^{-4}$
0·2	2	0·9334	−0·7301	18·3644	9·5774	$4\cdot1\times10^{-12}$	$9\cdot9\times10^{-12}$
	3	0·9334	−0·7301	18·3644	9·5774	$1\cdot2\times10^{-15}$	$4\cdot7\times10^{-16}$
	4	0·9334	−0·7301	18·3644	9·5774	$8\cdot3\times10^{-16}$	$2\cdot9\times10^{-16}$
	1	0·9334	−0·7301	18·3644	9·5774	$7\cdot5\times10^{-5}$	$1\cdot2\times10^{-5}$
0.1	2	0·9334	−0·7301	18·3644	9·5774	$1\cdot1\times10^{-12}$	$6\cdot0\times10^{-13}$
	3	0·9334	−0·7301	18·3644	9·5774	$9\cdot3\times10^{-16}$	$4\cdot5\times10^{-16}$
	4	0·9334	−0·7301	18·3644	9·5774	$9\cdot3\times10^{-16}$	$4\cdot5\times10^{-16}$

given by the FPM for different values of Δp will give different iterative formulae. The smaller Δp is, the more complex the corresponding iterative formulae are. Clearly, the formulae in the case $\Delta p = 1$ are the simplest of them.

We use the same example described in the previous section to show this point. At the beginning of the computation let $\sigma_0(\xi, h_s) = 0$ and $\zeta_0(x) = 0$. The new results obtained are used as initial solutions to make the next computation. Different values of Δp ($\Delta p = 1$, 0·2 and 0·1) are considered. The results are given in Table II.

From Table II it seems that the iterations for each value of Δp will converge. The more complex the iterative formulae are (i.e. the smaller Δp is), the faster the iteratation converges, but clearly more CPU time is needed.

It is interesting that if Δp is small enough, the numerical results will be accurate enough and no iteration is needed. Thus we can regard iterations as special cases of the FPM for large Δp.

There exist some other iterative formulae for non-linear water wave problems. The formulae given by Jensen *et al.*[6] are as follows:

$$g\phi_z + \tfrac{1}{2}\nabla\phi\nabla(\nabla\Phi\nabla\Phi) + \nabla\Phi\nabla(\nabla\Phi\nabla\phi - \nabla\Phi\nabla\Phi) + \frac{(\partial/\partial z)[g\Phi_z + \frac{1}{2}\nabla\Phi\nabla(\nabla\Phi\nabla\Phi)]}{g + \nabla\Phi\nabla\Phi_z}[\tfrac{1}{2}(U^2 - 2\nabla\Phi\nabla\phi + \nabla\Phi\nabla\Phi) - g\zeta_0] = 0, \tag{82}$$

$$\zeta = \zeta_0 + \frac{\frac{1}{2}(U^2 - 2\nabla\Phi\nabla\phi + \nabla\Phi\nabla\Phi) - g\zeta_0}{g + \nabla\Phi\nabla\Phi_z}, \tag{83}$$

where Φ and ζ_0 are old values and ϕ and ζ are new values.

Let us compare the above iterative formulae with the simplest ones given by the FPM in the case $\Delta p = 1$. It is well known that iterations are generally sensitive to the initial solutions and will diverge in some cases of strong non-linearity. The convergence region, the numerical maximum wave elevation (far downstream) and the maximum slope obtained by the different formulae are given in Table III.

According to Table III, the iterative formulae given by the FPM in the case $\Delta p = 1$ have a greater region of convergence than the iterative formulae (82) and (83). Note that $\Delta p = 1$ corresponds to the simplest case. In fact, the smaller Δp is, the more insensitive the corresponding iterative formulae are to the initial solutions.

Clearly, it is easy to use the basic ideas of the FPM to derive a family of iterative formulae for any reasonable non-linear problem, among which the simplest is in the case $\Delta p = 1$ and more complex formulae correspond to smaller Δp. If Δp is small enough, then the numerical results are accurate enough and no iteration is needed, although more CPU time is required.

In fact, the iterative formulae (82) and (83) can also be obtained from expressions (45) and (46).

Table III. Convergence regions for different iterative formulae

Iterative model	Convergence region ($\text{ft}^2\,\text{s}^{-1}$)	ζ_{max} (ft)	Max. slope (deg)
FPM ($\Delta p = 1$)	$-6{\cdot}49 \leqslant \Gamma/2\pi \leqslant 2{\cdot}45$	1·206	23·0
Reference 6	$-5{\cdot}88 \leqslant \Gamma/2\pi \leqslant 2{\cdot}13$	1·066	19·8

In (45) and (46) let $p=1$ and substitute ϕ_0 and ϕ by Φ; then one has

$$g\phi_z^{[1]}+\tfrac{1}{2}\nabla\phi^{[1]}\nabla(\nabla\Phi\nabla\Phi)+\nabla\Phi\nabla(\nabla\Phi\nabla\phi^{[1]})-\frac{\nabla\Phi\nabla\phi^{[1]}\partial\mathscr{R}(\Phi)/\partial z}{g+\nabla\Phi\nabla\Phi_z}$$
$$=-\mathscr{R}(\Phi)-\frac{[\mathscr{Z}(\Phi)-\zeta_0(x,y)]\partial\mathscr{R}(\Phi)/\partial z}{1+\nabla\Phi\nabla\Phi_z/g}, \tag{84}$$

Table IV. Maximum and minimum wave elevation (far downstream) for $U=10\,\text{ft}\,\text{s}^{-1}$ and $b=4{\cdot}5\,\text{ft}$

$\Gamma/2\pi$ ($\text{ft}^2\,\text{s}^{-1}$)	Third-order perturbation 11		Numerical results			
			Reference 11		Present method	
	ζ_{max} (ft)	ζ_{min} (ft)	ζ_{max} (ft)	ζ_{min} (ft)	ζ_{max} (ft)	ζ_{min} (ft)
−3·20	0·544	−0·511	0·64	−0·58	0·558	−0·438
−2·70	0·495	−0·339	0·60	−0·54	0·553	−0·436
−2·10	0·440	−0·335	0·50	−0·47	0·497	−0·401
−1·70	0·390	−0·326	0·43	−0·40	0·466	−0·382
−1·40	0·341	−0·298	0·37	−0·35	0·369	−0·317
−1·15	0·293	−0·263	0·30	−0·29	0·312	−0·275
−0·90	0·239	−0·220	0·25	−0·24	0·250	−0·226
0·90	0·308	−0·281	0·29	−0·28	0·305	−0·280
1·15	0·409	−0·361	0·38	−0·36	0·406	−0·362
1·40	0·517	−0·440	0·47	−0·44	0·514	−0·445
1·70	0·655	−0·534	0·59	−0·54	0·659	−0·548
2·20	0·908	−0·685	0·84	−0·72	0·959	−0·729
2·70	1·187	−0·848	1·24	−0·93	†	†
3·20	1·495	−1·082	†	†	†	†

† No convergence.

Table V. Wavelength (ft) (far downstream) for $U=10\,\text{ft}\,\text{s}^{-1}$ and $b=4{\cdot}5\,\text{ft}$

$\Gamma/2\pi$ ($\text{ft}^2\,\text{s}^{-1}$)	Third-order perturbation method[11]	Numerical results	
		Reference 11	Present method
−3·20	17·73	19·2	18·82
−2·70	18·24	19·3	18·83
−2·10	18·75	19·4	18·96
−1·70	19·02	19·5	19·11
−1·40	19·18	19·5	19·23
−1·15	19·30	19·5	19·32
−0·90	19·39	19·6	19·40
0·90	19·39	19·6	19·40
1·15	19·30	19·5	19·29
1·40	19·18	19·5	19·14
1·70	19·02	19·1	18·89
2·20	18·67	18·8	18·26
2·70	18·24	18·0	†
3·20	17·73	†	†

† No convergence.

$$\zeta^{[1]} = \frac{\mathscr{E}(\Phi) - \zeta_0(x, y) - \nabla\Phi\nabla\phi^{[1]}/g}{1 + \nabla\Phi\nabla\Phi_z/g}. \tag{85}$$

From the above expressions, substituting $\phi^{[1]}$ by $\phi - \Phi$ and $\zeta^{[1]}$ by $\zeta - \zeta_0$ respectively, one can obtain the same formulae as (82) and (83).

6. COMPARISON WITH OTHER RESULTS

In the case $U = 10$ ft s^{-1} and $b = 4{\cdot}5$ ft the 2D deep waves past a submerged vortex are researched by the numerical scheme described above. The numerical parameters used are $x_a/\lambda_0 = -3{\cdot}5$, $x_b/\lambda_0 = 1{\cdot}5$, $h_s = 1{\cdot}6$ ft and $N = 200$.

Table VI. Wave resistance (lb ft^{-1}) of 2D waves past a submerged vortex for $U = 10$ ft s^{-1} and $b = 4{\cdot}5$ ft

$\Gamma/2\pi$ (ft^2 s^{-1})	Perturbation results[11]			Numerical results	
	First-order	Second-order	Third-order	Reference 11	Present method
−3·20	13·92	10·40	4·04	5·53	3·616
−2·70	9·91	7·00	2·61	4·91	3·597
−2·10	5·99	4·13	2·26	3·54	3·011
−1·70	3·93	2·67	1·94	2·55	2·367
−1·40	2·66	1·94	1·55	1·91	1·809
−1·15	1·80	1·37	1·19	1·36	1·333
−0·90	1·10	0·88	0·81	0·88	0·884
0·90	1·10	1·41	1·33	1·22	1·321
1·15	1·80	2·48	2·23	2·08	2·251
1·40	2·66	3·95	3·40	3·15	3·476
1·70	3·93	6·34	5·10	4·84	5·351
1·90	4·91	8·38	6·40	6·19	6·894
2·20	6·58	12·23	8·57	8·73	9·642
2·50	8·49	17·17	10·96	11·76	†
2·70	9·91	21·15	12·66	14·04	†
3·20	13·92	33·97	16·97	†	†

† No convergence.

Table VII. 2D wave (far downstream) past a submerged vortex for $U = 10$ ft s^{-1} and $b = 4{\cdot}5$ ft

$\Gamma/2\pi$ (ft^2 s^{-1})	ζ_{max} (ft)	ζ_{min} (ft)	Max. slope (deg)	λ_w (ft)	R_w (lb ft^{-1})
−6·49	0·199	−0·172	3·6	19·64	0·526
−6·4	0·163	−0·140	2·8	19·70	0·329
−6·0	0·004	−0·002	0·5	†	0·010
−5·0	0·268	−0·217	4·6	19·17	0·863
−4·7	0·346	−0·278	5·9	19·12	1·425
−3·7	0·523	−0·412	9·0	18·88	3·180
2·30	1·039	−0·767	19·2	18·07	10·690
2·40	1·144	−0·792	21·5	17·68	11·728
2·45	1·206	−0·825	23·0	17·64	12·388
2·50	1·316	−0·848	25·8	17·37	12·942

† No numerical value of wavelength because of the too small wave height downstream.

The maximum and minimum wave elevation, wavelength (downstream) and wave resistance for different values of the vortex circulation $\Gamma/2\pi$ are given in Tables IV–VI respectively. The perturbation solutions is the third-order approximation for deep waves and the numerical results in finite water depth given in Reference 11 are also listed for comparison. The converged results for $\Gamma/2\pi < -3{\cdot}2\ \text{ft}^2\,\text{s}^{-1}$ and $\Gamma/2\pi > 2{\cdot}2\ \text{ft}^2\,\text{s}^{-1}$ are given in Table VII.

From Tables IV–VII it seems that for $|\Gamma/2\pi| < 1{\cdot}7\ \text{ft}^2\,\text{s}^{-1}$ the results given by the FPM, especially for the wavelength, are in better agreement with the perturbation solutions in he third-order approximation than with the numerical results given in Reference 11. For $|\Gamma/2\pi| > 1{\cdot}7\ \text{ft}^2\,\text{s}^{-1}$ we obtain results which are considerably different not only from the perturbation solutions in the third-order approximation but also from the numerical results given in

Table VIII. Maximum and minimum wave elevation and maximum slope of first crest

$\Gamma/2\pi$ ($\text{ft}^2\,\text{s}^{-1}$)	−6·49	−6·4	−6·0	−5·0	−4·7	−3·7	−3·2	−2·7
ζ_{max} (ft)	1·459	1·441	1·372	1·230	1·184	1·006	0·901	0·786
ζ_{min} (ft)	−0·147	−0·115	0·000	−0·160	−0·229	−0·385	−0·419	−0·424
Max. slope (deg)	29·7	25·8	21·7	17·5	16·6	14·3	13·1	11·7
$\Gamma/2\pi$ ($\text{ft}^2\,\text{s}^{-1}$)	−2·1	−1·9	−1·7	−1·4	−1·15	−0·9	0·9	1·15
ζ_{max} (ft)	0·633	0·579	0·523	0·436	0·362	0·285	0·302	0·401
ζ_{min} (ft)	−0·394	−0·376	−0·353	−0·313	−0·272	−0·224	−0·299	−0·385
Max. slope (deg)	9·8	8·9	8·1	6·9	5·8	4·6	5·5	7·2
$\Gamma/2\pi$ ($\text{ft}^2\,\text{s}^{-1}$)	1·40	1·70	1·90	2·20	2·30	2·40	2·45	2·50
ζ_{max} (ft)	0·509	0·652	0·759	0·881	0·950	1·029	1·191	1·291
ζ_{min} (ft)	−0·472	−0·578	−0·650	−0·724	−0·762	−0·799	−0·857	−0·878
Max. slope (deg)	9·2	11·7	13·7	16·1	17·4	19·17	22·7	25·1

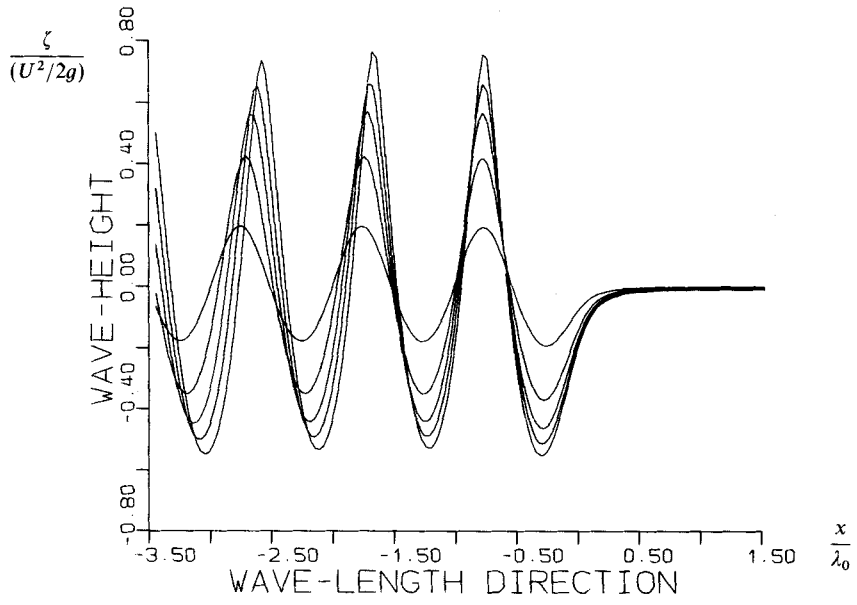

Figure 2. Wave elevation of 2D waves past positive circulations for $U = 10\ \text{ft}\,\text{s}^{-1}$, $b = 4{\cdot}5$ ft and infinite water depth. ζ_{max} increases with increasing $\Gamma/2\pi = 0{\cdot}90$, 1·70, 2·10, 2·30 and $2{\cdot}45\ \text{ft}^2\,\text{s}^{-1}$

Reference 11. It seems that perturbation solutions to a higher order of approximation should be given for flows with stronger non-linearity. Also, it seems that the water depth has a great influence on 2D waves past a submerged vortex, especially on their wavelength.

The maximum and minimum wave elevation and the maximum slope of the first crest are given in Table VIII. In the case of positive circulations the height of the first crest is nearly the same as those far downstream, but in the case of negative circulations the first crest is always higher.

Figures 2 and 3 show the wave elevation for different values of circulation. For positive circulations the elevation height of the first crest is nearly the same as those far downstream and all of them increase with increasing vortex circulation until the limit status is reached. For negative circulations the wave height of the first crest is always greater than those far downstream and increases with decreasing vortex circulation, whereas ζ_{max} far downstream has a crest value near $\Gamma/2\pi = -3{\cdot}2\ \mathrm{ft^2\,s^{-1}}$ and a trough value at $\Gamma/2\pi = -6\ \mathrm{ft^2\,s^{-1}}$ as shown in Figure 3. At $\Gamma/2\pi = -6\ \mathrm{ft^2\,s^{-1}}$ the height of the wave elevation far downstream is so small that it is nearly an isolated wave. In the case of negative circulations the maximum wave slope and maximum wave

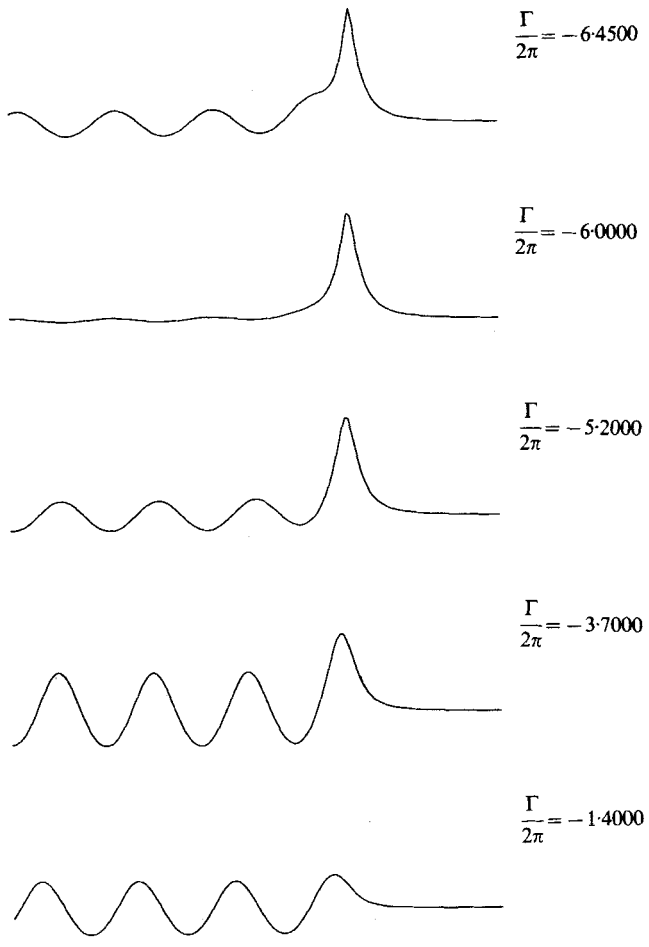

Figure 3. Wave elevation of 2D waves past negative circulations for $U = 10\ \mathrm{ft\,s^{-1}}$, $b = 4{\cdot}5$ ft and infinite water depth. From bottom to top the corresponding circulations are $\Gamma/2\pi = -1{\cdot}4,\ -3{\cdot}7,\ -5{\cdot}2,\ -6{\cdot}0$ and $-6{\cdot}45\ \mathrm{ft^2\,s^{-1}}$

elevation far downstream are much less than the theoretical limits. It is clear from Figure 3 that wave breaking will occur when the first crest is too high. According to the experiment of Salvensen,[13] wave breaking occurs at the first crest. Our numerical results support his experiment.

Stokes[14,15] showed that the limiting form of steady irrotational gravity waves possesses sharp crests containing an angle of 120°, i.e. a maximum slope of 30°. The limit of free surface elevation is

$$\zeta_{\text{lim}} = U^2/2g,$$

i.e. for $U = 10\,\text{ft s}^{-1}$, $\zeta_{\text{lim}} = 1{\cdot}54\,\text{ft}$.

Table IX. Steepest elevation (far downstream) of 2D deep gravity waves

			Numerical results	
	Theory	Experiment[13]	Reference 11	Present method
ζ_{lim}	$U^2/2g$	$0{\cdot}82U^2/2g$	$0{\cdot}87U^2/2g$	$0{\cdot}85U^2/2g$
Max. slope (deg)	30	25	24·4	25·8
$(H_w/\lambda_w)_{\text{max}}$	0·141–0·145	0·11	0·12	0·125

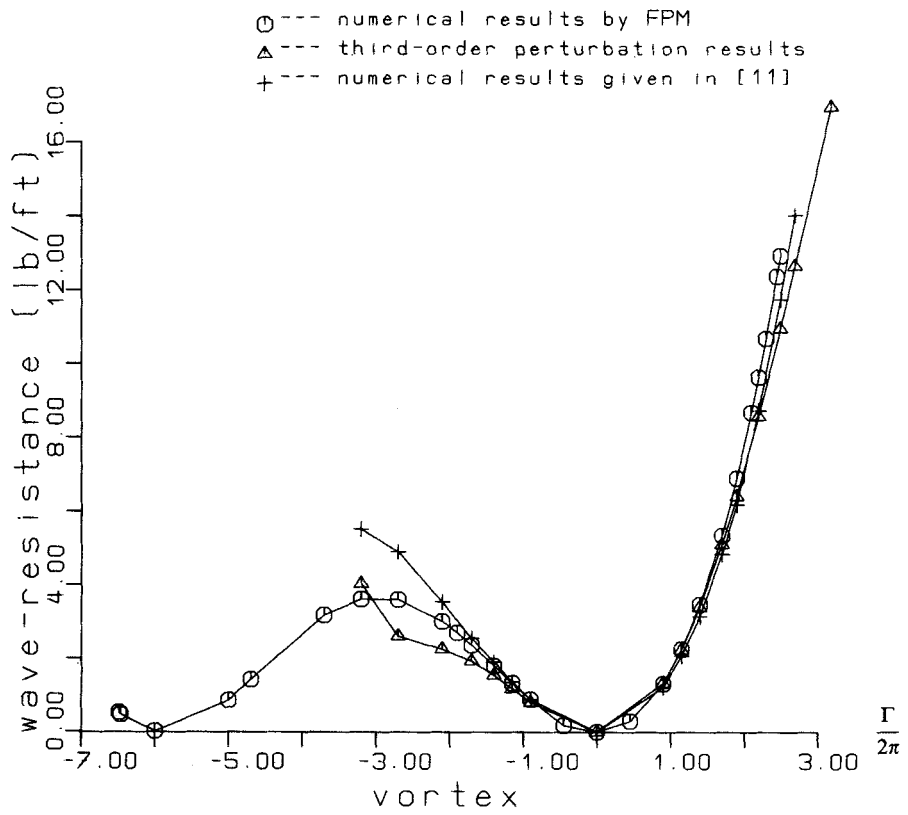

Figure 4. Wave resistance of 2D waves past a submerged vortex for $U = 10\,\text{ft s}^{-1}$ and $b = 4{\cdot}5\,\text{ft}$

The maximum ratio of wave height to length, H_w/λ_w, is given by Michell[16] as 0·142, by Thomas[17] as 0·145 and by Schwartz[18] as 0·141–0·142. The experiment by Salvensen[13] gives the maximum $H_w/\lambda_w = 0{\cdot}11$ for downstream waves, while the numerical maximum value given in Reference 11 is $H_w/\lambda_w = 0{\cdot}12$.

In the case $U = 10\ \text{ft s}^{-1}$ and $b = 4{\cdot}5$ ft the limit wave elevation is obtained at $\Gamma/2\pi = 2{\cdot}5\ \text{ft s}^{-1}$, with $\zeta_{max} = 1{\cdot}316$ ft, maximum $H_w/\lambda_w = 0{\cdot}125$ and maximum slope 25·8°. In comparison with Reference 11 we obtain a little steeper wave elevation as shown as Table IX. The limiting form of wave elevation for negative circulation is obtained in the case of $\Gamma/2\pi = -6{\cdot}49\ \text{ft}^2\,\text{s}^{-1}$, with the first crest $\zeta_{max} = 1{\cdot}459$ ft and maximum slope 29·7°, while the wave elevation far downstream is much more even. It is interesting that the limiting form of wave elevation for negative circulation is very different from that for positive circulation, as shown in Figures 2 and 3.

Figure 4 shows the wave resistance in the case $U = 10\ \text{ft s}^{-1}$ and $b = 4{\cdot}5$ ft. For $\Gamma > 0$ the wave resistance increases with increasing vortex circulation, but for $\Gamma < 0$ the curve of wave resistance is very different; there exist a crest and also a trough in the region of negative circulation. At $\Gamma/2\pi = -6\ \text{ft}^2\,\text{s}^{-1}$ the wave resistance is nearly zero, while the corresponding wave elevation is nearly an isolated wave. For $\Gamma/2\pi < -6\ \text{ft}^2\,\text{s}^{-1}$ the wave resistance increases until the first crest of wave elevation is too high and then numerical wave breaking occurs. These very interesting results have not been reported in Reference 11.

Similarly to the wave resistance, the wavelengths in the case of negative circulations are also considerably different from those in the case of positive circulations, as shown in Figure 5. For

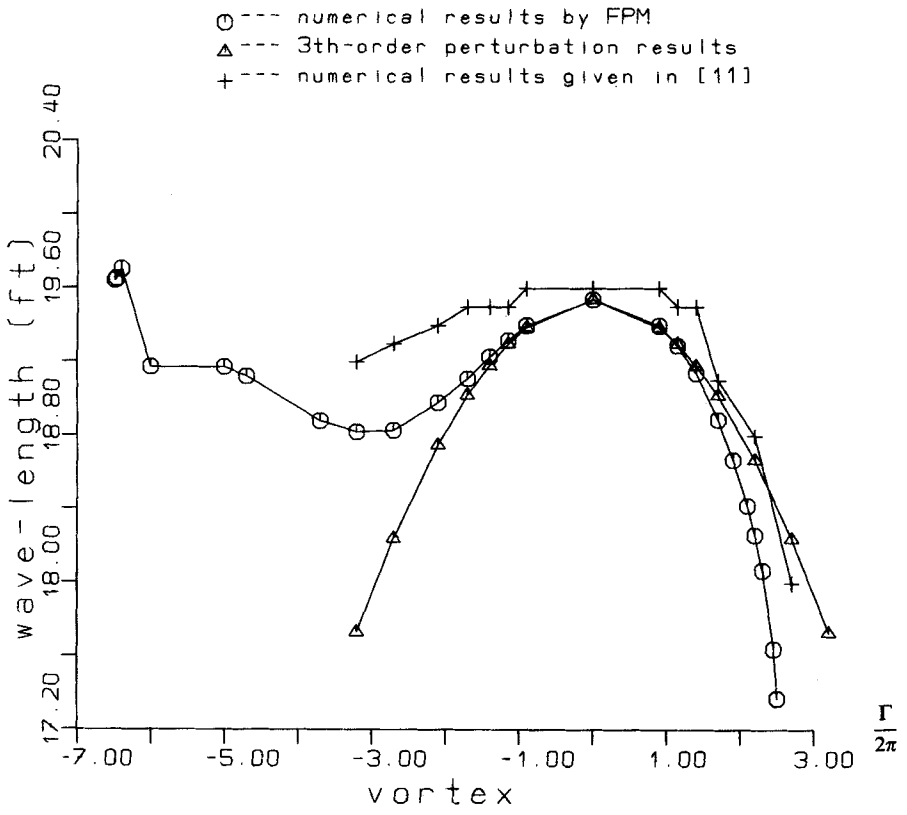

Figure 5. Wavelength of 2D waves past a submerged vortex for $U = 10\ \text{ft s}^{-1}$ and $b = 4{\cdot}5$ ft

positive circulation the wavelength always decreases with increasing vortex circulation. For negative circulation the wavelength decreases at first but begins to *increase* later. This result is interesting.

The wave resistance is nearly zero in the case $\Gamma/2\pi = -6\ \mathrm{ft}^2\,\mathrm{s}^{-1}$. Perhaps more attention should be paid to this interesting result, which can be obtained by the FPM but not by the iterative formulae (82) and (83). We know that a 2D submerged wing or streamlined foil can be substituted approximately by a submerged vortex. Thus it seems that the wave resistance of a submerged 2D wing or streamlined foil might be zero in some cases. Are there any applications of this result in engineering if it also holds true for a 3D wing or streamlined foil? Could we use submerged wings or streamlined foils in the fore of a ship to reduce its wave resistance? Clearly a submerged vortex is too crude a model for a submerged 3D wing or streamlined foil. 3D models close to practical problems should be used in order to obtain more accurate results with practical meaning, and naturally experiments should be done. It seems valuable to investigate this problem thoroughly.

7. DISCUSSION AND CONCLUSION

The basic idea of the finite process method is to discretize an original non-linear problem into a finite number of linear problems in a continuous mapping domain $p \in [0, 1]$. The finer this discretization is, i.e. the smaller Δp is, the more accurate the numerical results are. If Δp is small enough, then the numerical results are accurate enough, but clearly more CPU time is needed. In this way we can avoid the use of iterative techniques to solve non-linear problems.

On the other hand, the formulae of the FPM at any definite values of $\Delta p = 1/n_p$ can also be used as iterative formulae. This gives a family of iterative models. The smaller Δp is, the more complex but more insensitive to initial solutions the corresponding iterative formulae are. If Δp is small enough, then the results are accurate enough and no iteration is needed. Thus we can regard iterative formulae as special cases of the FPM for large Δp.

Every method has its good and bad points: simpler iterative formulae are more sensitive to initial solutions; on the other hand, more complex formulae need more CPU time. For weak non-linear problems, simpler formulae with large Δp, e.g. $\Delta p = 1$ or 0·5, can be used. However, for more strongly non-linear problems, formulae with smaller Δp seem be needed in order to obtain converged results, and naturally more CPU time is needed in these cases. It seems that we must make more effort for strongly non-linear problems.

ACKNOWLEDGEMENTS

Sincere thanks are due to Professor H. Söding for his suggestions. This work is supported by DAAD and the computer time is freely provided by the Institute of Shipbuilding, University of Hamburg.

APPENDIX: NOMENCLATURE

$(e_d)_{max}$	maximum non-dimensional error of dynamic condition of free surface
$(e_k)_{max}$	maximum non-dimensional error of kinematic condition of free surface
$f_1(p)$	first-type process function defined by expression (7)
$f_2(p)$	second-type process function defined by expression (8)
g	gravitational acceleration
$\mathscr{L}[\phi(x, y, z)]$	auxiliary function defined by expression (6)
H_w	wave height

p	process-independent variable
$\mathscr{R}[\phi(x, y, z)]$	auxiliary function defined by expression (5)
R_w	wave resistance given by expression (77)
$\mathscr{S}[\phi(x, y, z; p); p]$	auxiliary function defined by expression (40)
$\mathscr{T}[\phi(x, y, z; p); p]$	auxiliary function defined by expression (41)
U	velocity of body

Greek letters

$\phi(x, y, z)$	velocity potential function
$\phi_0(x, y, z)$	initial velocity potential function
$\phi_f(x, y, z)$	final velocity potential function
$\phi(x, y, z; p)$	mapping of $\phi(x, y, z)$, called zero-order process of $\phi(x, y, z)$
$\phi^{[1]}(x, y; p)$	first-order process derivatives of $\phi(x, y, z; p)$
$\zeta(x, y)$	wave elevation
$\zeta_0(x, y)$	initial wave elevation
$\zeta_f(x, y)$	final wave elevation
$\zeta(x, y; p)$	mapping of $\zeta(x, y)$, called zero-order process of $\zeta(x, y)$
$\zeta^{[1]}(x, y; p)$	first-order process derivatives of $\zeta(x, y; p)$
Ω	fluid domain

REFERENCES

1. C. W. Dawson, 'A practical computer method for solving ship-wave problems', *Proc. Second Int. Conf. on Numerical Ship Hydrodynamics*, 1977. University of California, Berkeley, 1977, pp. 30–38.
2. J. Hess and A. M. O. Smith, 'Calculation of non-lifting potential flow about three-dimensional bodies', *Douglas Aircraft Company Rep. ES 40622*, 1962.
3. E. Campana, F. Lalli and U. Bulgarelli, 'A boundary element method for a nonlinear free surface problem', *Int. j. numer. methods fluids*, **9**, 1195–1206 (1989).
4. O. Dauber and A. Dulieu, 'A numerical approach of the nonlinear wave resistance problem', *Proc. Third Int. Conf. on Numerical Ship Hydrodynamics*, Palais des Congrès Paris, 1981, pp. 73–80.
5. J. L. Hess, 'Progress in the calculation of the nonlinear free-surface problems by surface-singularity techniques', *Proc. Second Int. Conf. on Numerical Ship Hydrodynamics*, University of California, Berkeley, 1977, pp. 278–284.
6. G. Jensen, Z. X. Mi and H. Söding, 'Rankine source methods for numerical solutions of the steady wave resistance problem', *Proc. 16th Symp. on Naval Hydrodynamics*, University of California, Berkeley, CA, 1986, pp. 575–582.
7. H. Maruo and S. Ogiwara, 'A method of computation for steady ship-waves with nonlinear free-surface conditions', *Proc. Fourth Int. Conf. on Numerical Ship Hydrodynamics*, Office of Naval Research, Department of The Navy, Washington, D.C., 1985, pp. 218–233.
8. F. Xia, 'Numerical calculations of ship flows, with special emphasis on the free surface potential flow', Chalmers University of Technology, Göteborg, 1986 (ISBN 91-7032-248-1).
9. J. W. Macarthur, 'Semidirect finite difference methods for solving the Navier–Stokes and energy equations', *Int. j. numer. methods fluids*, **9**, 325–340 (1989).
10. S. J. Liao, 'A general numerical method for solution of gravity waves. Part 1: 2D steep gravity waves in shallow water', *Int. j. numer. methods fluids*, **12**, 727–745 (1991).
11. N. Salvesen and C. Kerczek, 'Comparison of numerical and perturbation solutions of two-dimensional nonlinear water-wave problems', *J. Ship Res.*, **20**, 160–170 (1976).
12. J. Wehausen, 'The wave resistance of ships', *Adv. Appl. Mech.*, **13**, 93–245 (1973).
13. N. Salvesen, 'Second-order wave theory for submerged two-dimensional bodies', *Proc. ONR 6th Naval Hydrodynamics Symp.*, Office of Naval Research, Department of The Navy, Washington, D.C., 1966, pp. 595–628.
14. G. G. Stokes, 'On the theory of oscillatory waves', *Trans. Camb. Phil. Soc.*, **8**, 441–455 (1847).
15. G. G. Stokes, 'On the highest waves of uniform propagation', *Proc. Camb. Phil. Soc.* **4**, 361–365 (1883).
16. J. H. Michell, 'The highest waves of water', *Phil. Mag.* **36**, 430–437 (1893).
17. J. W. Thomas, 'Irrotational gravity waves of finite height: a numerical study', *Mathematika*, **15**, 139–148 (1968).
18. L. W. Schwartz, 'Computer extension and analytic continuation of Stokes expansion for gravity waves', *J. Fluid Mech.*, **62**, 553–578 (1974).